Instability in active balancing control of dc bus voltages in VSC converters interconnected via multi-winding transformers

Duro Basic, Sami Siala
General Electric, Power Conversion
18 Avenue de Québec, Villebon-Sur-Yvette, 91140 France
E-Mail: duro.basic@ge.com, sami.siala@ge.com
URL: https://www.gepowerconversion.com/

Keywords

«Parallel converters», « Pulse-Width-Modulated (PWM) converters », «Interleaving», «Grid connected converters»

Abstract

In high power applications, 3-phase ac/dc Voltage Source Converters (VSCs) are paralleled to increase the overall aggregated converter power rating, number of voltage steps, effective switching frequency and control bandwidth. For this, the interleaved Pulse Width Modulation (PWM) and current limiting converter paralleling inductors are utilized. Interphase Transformers (ITRs) or Multi-Winding Transformers (MWTs) are often adopted for the converter paralleling because they provide large inductances for the currents flowing among the converters while introduce relatively lower leakage inductances for the currents flowing from the converters to the power grid. However, large asymmetries in the inductances created by magnetic coupling in these transformers make it difficult to independently control active power flows in the converters. Thus, if the converter dc buses are not interconnected, instabilities in the active balancing control of the converter dc bus voltages are possible in certain operational conditions. In this paper MWT model and effects of magnetic coupling introduced by it on controllability of the power flows among the converters are presented. Operational condition leading to instability of the active balancing control is theoretically defined and validated in simulations.

Introduction

In high power applications, a number *N* of identical 3-phase ac/dc VSCs can be connected in parallel to increase power rating of the aggregated converter [1]-[4]. To increase the effective switching frequency, control bandwidth and reduce switching harmonics in the output voltage, the PWM carriers of the individual converters are mutually interleaved [5]. Thus, the converter paralleling requires utilization of coupling inductors to limit high frequency currents flowing among the converters which are produced by non-synchronous PWM switching. With the interleaved PWM, large paralleling inductors are needed to limit the current PWM switching harmonics [6]. To avoid large voltage drops across the paralleling inductors, ITRs can be used which provide large magnetizing inductance for the currents flowing among converters (cross currents) while introducing a negligible leakage inductance for the currents flowing from the converters to the power grid (cumulative currents) [4],[7]. Alternatively, the converters can be paralleled via MWTs as shown in Fig. 1, where the transformer leakage inductances provide the required paralleling inductances, grid-converter voltages matching and isolation [1] [2]. In such systems the MWT is normally designed to maximize the leakage inductances among the secondary windings [8] to minimize the PWM cross currents flowing among the secondary windings. In the converter systems with isolated or stacked dc busses (Fig. 1) the dc bus voltages of individual converters may diverge due to slight system imbalances. To ensure balanced dc bus voltages in all converters, the net active power absorption in each converter dc bus must be actively controlled, typically via control of the cross currents. However, unexpected instabilities in the dc bus voltage balancing control may be encountered in operatorial points characterised by low capacitive power factors. These instabilities have been previously reported in the STATCOM applications [9] with the converters paralleled via ITRs [4]. These instabilities have been linked in [9] to extremely large asymmetries of the inductances in the cumulative and cross current paths created by the converter paralleling via ITRs. In this paper it will be shown that such type of instabilities can also appear in the converter systems paralleled via MWTs.

The paper is organized as follows. Initially, modelling of MWTs using equivalent polygonal networks and coupled inductors is presented. Then the multi converter system model is derived using decompositions of the converter voltages and currents into so called cumulative components (defining power exchange with the power grid) and cross components (related to the cross currents and power flows among the converters). Based on such decompositions a multi-variable model is derived which describes cross-power flows among the converters in function of the cross currents. This multi-variable model considers the magnetic cross-coupling introduced by MWTs and gives an insight into the origin of the balancing control instability and allows quantification of the critical capacitive cumulative reactive current injection which initiates it. Finally, results of simulations of an example system are presented to validate the theoretical results and lustrate onset of the instability.

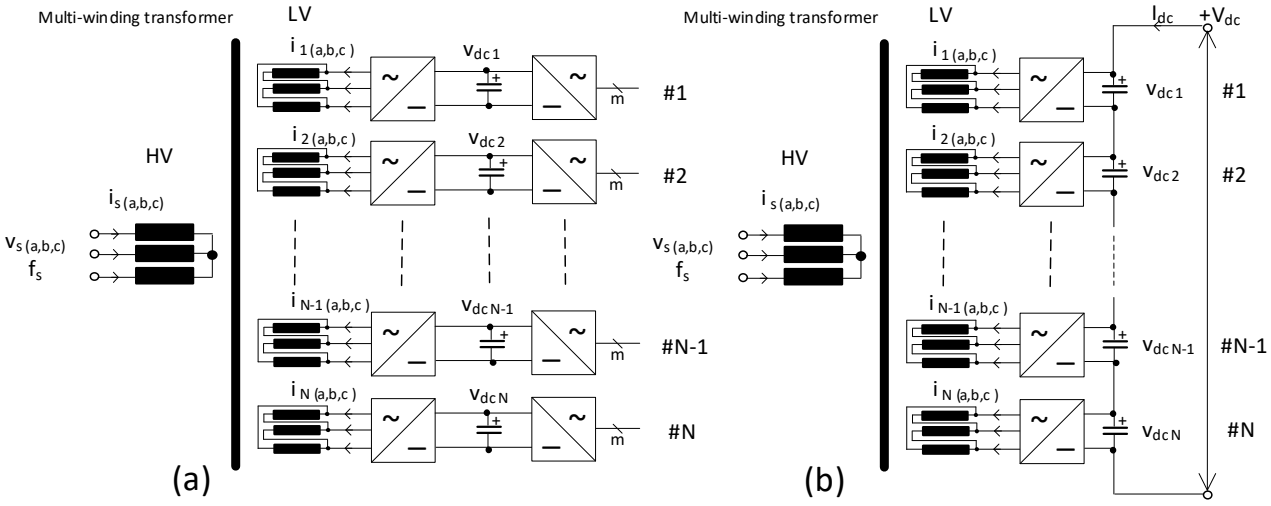

Fig. 1: Converter system based on *N* VSC converters interconnected using MWT with (a): individual back-back connected ac/dc/ac converters and (b): stacked ac/dc converters and common dc link.

Modelling of multi-winding transformers

The leakage impedances of MWTs with a primary (Higher Voltage, HV) and *N* secondary (Lower Voltage, LV) windings can be modelled by a polygonal network shown in Fig. 2 [10] [11]. The network parameters can be deduced from a matrix of short circuit voltages (shown in Table 1) which defines the short circuit voltages or reactances among all combinations of two windings in MWTs with *N* secondary windings [12]. This matrix can be obtained via calculations (in the transformer design phase) or in the short circuit tests (in the transformer validation phase). In Table 1 it is assumed that one winding (placed in a particular row) is energised while other winding (placed in a particular column) is short circuited. The voltage across the energised winding is increased until nominal current in that winding is reached. The short circuit voltage is then recorded in the table (at the intersection of the row /column corresponding to the position of the energised/short, circuited winding). The short circuit voltages in the matrix are typically expressed in per unit system where the base apparent power can be nominal apparent power of a single LV winding or power of the overall transformer (the base apparent power *Sb* should be clearly stated in the table). Dimension of the Table 1 depends on number of LV windings (*N*).

Table 1: Short circuit voltages $V_{SC\,LVi\text{-}HV}$/ $V_{SC\,LVi\text{-}LVj}$ (p.u. impedances $X_{SC\,LVi\text{-}HV}$/ $X_{SC\,LVi\text{-}LVj}$) which define magnetic couplings between all combinations of two windings in a MWT with *N* secondary windings.

Sb Base		Short-circuited Side						
		HV	LV1	LV2	LV3	LV4	LV5	LV6
Widing submited to rated current	HV		N=1					
	LV1	$Vsc\%_{LV1\text{-}HV}$		N=2				
	LV2	$Vsc\%_{LV2\text{-}HV}$	$Vsc\%_{LV2\text{-}LV1}$		N=3			
	LV3	$Vsc\%_{LV3\text{-}HV}$	$Vsc\%_{LV3\text{-}LV1}$	$Vsc\%_{LV3\text{-}LV2}$		N=4		
	LV4	$Vsc\%_{LV4\text{-}HV}$	$Vsc\%_{LV4\text{-}LV1}$	$Vsc\%_{LV4\text{-}LV2}$	$Vsc\%_{LV4\text{-}LV3}$		N=5	
	LV5	$Vsc\%_{LV5\text{-}HV}$	$Vsc\%_{LV5\text{-}LV1}$	$Vsc\%_{LV5\text{-}LV2}$	$Vsc\%_{LV5\text{-}LV3}$	$Vsc\%_{LV5\text{-}LV4}$		N=6
	LV6	$Vsc\%_{LV6\text{-}HV}$	$Vsc\%_{LV6\text{-}LV1}$	$Vsc\%_{LV6\text{-}LV2}$	$Vsc\%_{LV6\text{-}LV3}$	$Vsc\%_{LV6\text{-}LV4}$	$Vsc\%_{LV6\text{-}LV5}$	

The Table 1 can be viewed as a generalisation of the standard short circuit voltage specification of two-winding transformers. For two winding transformers with single LV winding, there is only a single short circuit voltage value (Vsc% $_{\text{LV1-HV}}$). For 3 winding transformers with 2 LV secondaries, 3 short circuit voltages are needed to characterise all leakage reactances in the transformer. In a general case of a N+1 winding transformer with N LV windings, $N(N+1)/2$ short circuit voltages are needed.

The short circuit voltages in Table 1 are directly related to the short circuit impedances between all pairs of two winding ($X_{SC\ LVi\text{-}HV}$ or $X_{SC\ LVi\text{-}LVj}$). From them it is possible to identify all parameters of the polygonal network in Fig. 2, which interconnects all nodes/winding terminals. The winding resistances can be added to the inductance network to complete MWT model.

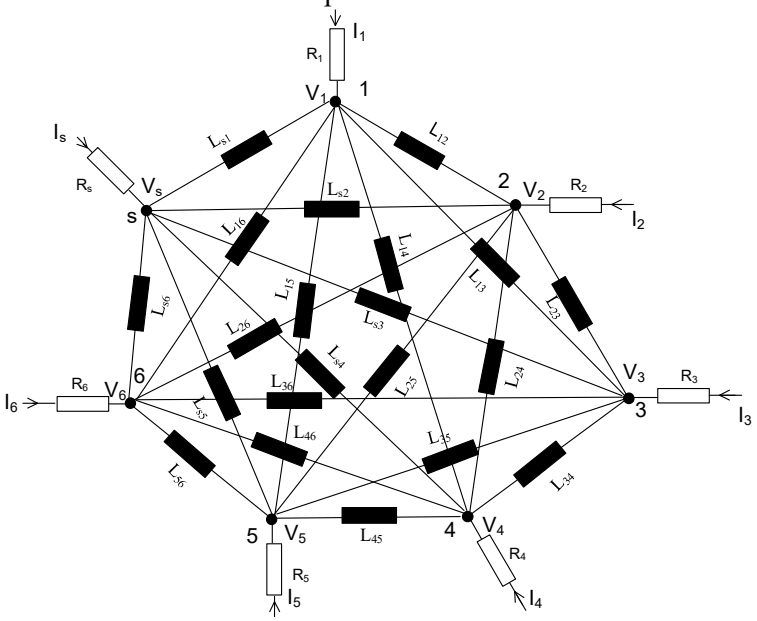

Fig. 2*:* Example of the equivalent polygonal scheme of a HV+6 LV MWT. All windings are referred to same voltage level (typically the secondary windings voltage level).

In the polygonal network Fig. 2 the winding terminal voltages and currents can be linked by the node equations written in the matrix form for the entire transformer model (N+1 nodes):

$$[I_t] = [Y_t]_{(N+1)\times(N+1)}\,[V_t] \tag{1}$$

In (1) $[I_t]$ is a vector containing all MWT windings currents, $[V_t]$ is a vector of all MWT windings voltages and $[Y_t]_{(N+1)\times(N+1)}$ is MWT admittance matrix. All reactances, voltages and currents are referred to same voltage (usually LV voltage) assuming equivalent star connection. In developed form, the MWT nodes matrix equation can be deduced by inspection from Fig. 2. It has the following general form:

$$\begin{bmatrix} I_s \\ I_1 \\ I_2 \\ - \\ - \\ I_{N-1} \\ I_N \end{bmatrix} = \begin{bmatrix} \frac{1}{jX_{ss}} & -\frac{1}{jX_{s1}} & -\frac{1}{jX_{s2}} & - & - & -\frac{1}{jX_{s(N-1)}} & -\frac{1}{jX_{sN}} \\ -\frac{1}{jX_{1s}} & \frac{1}{jX_{11}} & -\frac{1}{jX_{12}} & - & - & -\frac{1}{jX_{1(N-1)}} & -\frac{1}{jX_{1N}} \\ -\frac{1}{jX_{2s}} & -\frac{1}{jX_{21}} & \frac{1}{jX_{22}} & - & - & -\frac{1}{jX_{2(N-1)}} & -\frac{1}{jX_{2N}} \\ - & - & - & - & - & - & - \\ & & & & & & \\ - & - & - & - & - & - & - \\ -\frac{1}{jX_{(N-1)s}} & -\frac{1}{jX_{(N-1)1}} & -\frac{1}{jX_{(N-1)2}} & - & - & \frac{1}{jX_{(N-1)(N-1)}} & -\frac{1}{jX_{(N-1)N}} \\ -\frac{1}{jX_{Ns}} & -\frac{1}{jX_{N1}} & -\frac{1}{jX_{N2}} & - & - & -\frac{1}{jX_{N(N-1)}} & \frac{1}{jX_{NN}} \end{bmatrix} \begin{bmatrix} V_s \\ V_1 \\ V_2 \\ - \\ - \\ V_{N-1} \\ V_N \end{bmatrix} \tag{2}$$

where X_{ij} for $i = s,1..N$ and $j = s,1..N$ are reactance defined as follows:

- for $i \neq j$, the matrix element is simply the admittance between two nodes:

$$Y_{ij} = -\frac{1}{jX_{ij}} \qquad \text{where} \qquad Y_{ji} = Y_{ij} \qquad X_{ij} = \omega_s L_{i,j} \tag{3}$$

- The diagonal elements in the admittance matrix $(i = j)$ are a negative sum of all admittances connected to corresponding nodes:

$$\frac{1}{jX_{ss}} = \frac{1}{jX_{s1}} + \frac{1}{jX_{s2}} + . \quad . + \frac{1}{jX_{s(N-1)}} + \frac{1}{jX_{sN}}$$

$$\frac{1}{jX_{11}} = \frac{1}{jX_{1s}} + \frac{1}{jX_{12}} + . \quad . + \frac{1}{jX_{1(N-1)}} + \frac{1}{jX_{1N}}$$

--

$$\frac{1}{jX_{NN}} = \frac{1}{jX_{Ns}} + \frac{1}{jX_{N1}} + \frac{1}{jX_{N2}} + . \quad . + \frac{1}{jX_{N(N-1)}} \tag{4}$$

When only the leakage inductances and related couplings are considered with the magnetizing inductances neglected, the polygonal network is not connected to the ground reference node. Then, as only N winding currents are independent, it is possible to reduce dimension of the model by grounding the primary node (V_s=0). It leads to a reduced equation (5):

$$[I_{LV}] = [Y_t]_{N\times N}[V_{LV}] \tag{5}$$

where the reduced admittance matrix with matrix dimensions $N\times N$ can be deduced from $[Y_t]_{(N+1)\times(N+1)}$ (by omitting the 1st column and 1st row in (2)):

$$[Y_t]_{N\times N} = \begin{bmatrix} \frac{1}{jX_{11}} & -\frac{1}{jX_{12}} & - & - & - & -\frac{1}{jX_{1(N-1)}} & -\frac{1}{jX_{1N}} \\ -\frac{1}{jX_{21}} & \frac{1}{jX_{22}} & - & - & - & -\frac{1}{jX_{2(N-1)}} & -\frac{1}{jX_{2N}} \\ - & - & - & - & - & - & - \\ - & - & - & - & - & - & - \\ - & - & - & - & - & - & - \\ -\frac{1}{jX_{(N-1)1}} & -\frac{1}{jX_{(N-1)2}} & - & - & - & \frac{1}{jX_{(N-1)(N-1)}} & -\frac{1}{jX_{(N-1)N}} \\ -\frac{1}{jX_{N1}} & -\frac{1}{jX_{N2}} & - & - & - & -\frac{1}{jX_{N(N-1)}} & -\frac{1}{jX_{NN}} \end{bmatrix} \tag{6}$$

The matrix $[Y_t]_{N\times N}$ is invertible, and the leakage flux related reactance matrix $[X_\sigma]$ can be found:

$$[V_{LV}] = [X_\sigma][I_{LV}] \qquad \text{where} \qquad [X_\sigma] = [Y_t]_{N\times N}^{-1} \tag{7}$$

$$\begin{bmatrix} V_1 \\ V_2 \\ - \\ \\ - \\ V_{N-1} \\ V_N \end{bmatrix} = \begin{bmatrix} jX_{\sigma 11} & jX_{\sigma 12} & - & jX_{\sigma 1(N-1)} & jX_{\sigma 1N} \\ jX_{\sigma 21} & jX_{\sigma 22} & - & X_{\sigma 2(N-1)} & X_{\sigma 2N} \\ - & & - & - & - \\ & & - - - & & \\ - & & - & - & - \\ jX_{\sigma (N-1)1} & jX_{\sigma (N-1)2} & - & X_{\sigma (N-1)(N-1)} & X_{\sigma (N-1)N} \\ jX_{\sigma N1} & jX_{\sigma N2} & - & X_{\sigma N(N-1)} & X_{\sigma NN} \end{bmatrix} \begin{bmatrix} I_1 \\ I_2 \\ - \\ \\ - \\ I_{N-1} \\ I_N \end{bmatrix} \tag{8}$$

Introduction of the leakage reactance matrix (8) is important because its elements can be deduced from the short circuit voltage/impedance data provided in Table 1. The off-diagonal elements in $[X_\sigma]$ are found from Table 1 considering mutual coupling between LV windings in the short circuit tests:

$$X_{\sigma ij} = \frac{X_{sc\,LVi-HV} + X_{sc\,LVj-HV} - X_{sc\,LVi-LVj}}{2} \qquad i = 2...N \qquad j = 1...i-1 \tag{9}$$

The diagonal elements are equal the short circuit impedance between the LV windings and primary:

$$X_{\sigma ii} = X_{sc\,LVi-HV} \qquad i = 1...N \tag{10}$$

From the leakage reactance matrix $[X_\sigma]$ the leakage inductance matrix is $[L_\sigma] = 1/(j\omega_s)[X_\sigma]$. The $[L_\sigma]$ matrix is very important as it defines inductances seen between different LV windings in a MWTs. To minimize high frequency PWM cross currents, it is desirable to have as high as possible leakage inductances. Further, from the leakage reactance matrix $[X_\sigma]$ it is possible to reconstruct the full MWT model (2) which can be easily implemented in power electronics circuit simulators. For that the reduced admittance matrix $[Y_t]_{N\times N}$ is firstly found from (7):

$$[Y_t]_{N\times N} = [X_\sigma]^{-1} \tag{11}$$

Then, from the admittance matrix $[Y_t]_{N\times N}$ the full MWT model admittance matrix $[Y_t]_{(N+1)\times(N+1)}$ can be constructed. The missing elements of the 1st column/row is obtained from the elements of the matrix $[Y_t]_{N\times N}$ (as sum of the row /column elements in the floating admittance matrix $[Y_t]_{(N+1)\times(N+1)}$ is zero):

$$\begin{aligned}
&\frac{1}{X_{1s}} = \frac{1}{X_{s1}} = -\left(Y_{t\,11} + Y_{t\,12} + . \quad . + Y_{t\,1(N-1)} + Y_{t\,1N}\right)\\
&\frac{1}{X_{2s}} = \frac{1}{X_{s2}} = -\left(Y_{t\,21} + Y_{t\,22} + . \quad . + Y_{t\,2(N-1)} + Y_{t\,2N}\right)\\
&\cdots\\
&\frac{1}{X_{Ns}} = \frac{1}{X_{sN}} = -\left(Y_{t\,N1} + Y_{t\,N2} + . \quad . + Y_{t\,N(N-1)} + Y_{t\,NN}\right)\\
&\frac{1}{X_{ss}} = -\left(\frac{1}{X_{s1}} + \frac{1}{X_{s2}} + . \quad . + \frac{1}{X_{s(N-1)}} + \frac{1}{X_{sN}}\right)
\end{aligned} \tag{12}$$

In this way the MWT admittance matrix $[Y_t]_{(N+1)\times(N+1)}$ (2) is completed. For simulation studies using the circuit simulation software (like PLECS) it is convenient to express the transformer model in the coupled reactance (inductance) form:

$$[V_t] = [Y_t]_{(N+1)\times(N+1)}^{-1}[I_t] \tag{13}$$

However, it is not possible to find an inverse of the matrix $[Y_t]_{(N+1)\times(N+1)}$ because it is singular (its added row and column are found using linear combinations of other rows and columns). The problem can be resolved by attaching a shunt magnetizing reactance X_m at all or to just a single (let say primary winding) node. In the latter case, it leads to the following correction of the HV node admittance:

$$\frac{1}{X_{1s}} = \frac{1}{X_{1s}} + \frac{1}{X_m} \tag{14}$$

With it, the matrix $[Y_t]_{(N+1)\times(N+1)}$ becomes invertible and the coupled inductor matrix can be finally found:

$$[L_t] = \frac{1}{j\omega_s}[Y_t]_{(N+1)\times(N+1)}^{-1} \tag{15}$$

In the simulations with the actual voltage levels, it is possible to incorporate the transformer voltage transformation ratios defined by the ratios of the winding nominal (indexed by *n*) voltages and currents:

$$[T_v] = diag\left(\left[\frac{V_{sn}}{V_b} \;\; \frac{V_{1n}}{V_b} \;\; \frac{V_{2n}}{V_b} \;\; - \;\; - \;\; \frac{V_{(N-1)n}}{V_b} \;\; \frac{V_{Nn}}{V_b}\right]\right) \quad [T_i] = diag\left(\left[\frac{I_b}{I_{sn}} \;\; \frac{I_b}{I_{1n}} \;\; \frac{I_b}{I_{2n}} \;\; - \;\; - \;\; \frac{I_b}{I_{(N-1)n}} \;\; \frac{I_b}{I_{Nn}}\right]\right) \tag{16}$$

either via ideal transformers or directly via the coupled inductor matrix. In the direct approach, the final coupled inductor matrix of the MWT, which incorporates the transformation ratios, is:

$$[L_{MWT}] = [T_v][L_t][T_i] \tag{17}$$

Modelling of multi converter systems interconnected via MWTs

In theoretical analysis of a multi converter systems created by paralleling of N converters it is useful decompose the converter (LV side) voltage and current vectors:

$$\left[v\right]=\left[v_1 \quad v_2 \quad v_3 \quad \cdots \quad v_{(N-1)} \quad v_N\right]^T \qquad \left[i\right]=\left[i_1 \quad i_2 \quad i_3 \quad \cdots \quad i_{(N-1)} \quad i_N\right]^T \tag{18}$$

into the cumulative components defining interaction between the aggregated converter and power grid:

$$v_\Sigma = 1/N\sum_{i=1}^{N} v_i \qquad i_\Sigma = 1/N\sum_{i=1}^{N} i_i = i_s/N \qquad i=1{:}N \tag{19}$$

and the cross or circulating components defining interactions among the converters:

$$\left[\Delta v\right]=\left[v\right]-v_\Sigma \qquad \left[\Delta i\right]=\left[i\right]-i_\Sigma \qquad i=1{:}N \tag{20}$$

Considering that the diagonal elements in the admittance matrix (2) are negative sums of all admittances connected to the nodes, the first row in (2) links the converter cumulative voltage components and the grid voltage V_s via a simple scalar reactance (inductance) X_t (L_t) which represents the transformer short circuit impedance obtained in the test with all LV windings short circuited:

$$jX_t=\left(\frac{1}{jX_{s1}}+\frac{1}{jX_{s2}}+\cdots+\frac{1}{jX_{s(N-1)s}}+\frac{1}{jX_{sN}}\right)^{-1} \qquad L_t = X_t/\omega_s \tag{21}$$

If the winding resistances are neglected, the following voltage equation describing the cumulative system is obtained:

$$v_\Sigma - v_s \approx L_t\frac{d}{dt}\left(Ni_\Sigma\right) \qquad \text{in steady state:} \qquad V_\Sigma - V_s \approx j\omega_s L_t NI_\Sigma \tag{22}$$

The cross currents and voltages can be linked via the cross-coupling inductance matrix $\left[L_\sigma\right]$ (under assumption of symmetrical distribution of short circuit currents in LV windings in the short circuit test supplied from the HV side and with all LV windings shorted):

$$\left[\Delta v\right]\approx\left[L_\sigma\right]\frac{d}{dt}\left[\Delta i\right] \qquad \text{in steady state} \qquad \left[\Delta v\right]\approx j\omega_s\left[L_\sigma\right]\left[\Delta i\right]=\left[X_\sigma\right]\left[\Delta i\right] \tag{23}$$

The cumulative mode (fundamental) current components define the active and reactive power flows between the aggregated converter and the grid. Thus, the active cumulative current component ($I_{\Sigma d}$, in phase with the grid voltage V_s) is used for control of the total active power flow and stored energy in the converter dc bus capacitors of all converters. The reactive cumulative current component ($I_{\Sigma q}$, in quadrature to the grid voltage V_s) defines the total reactive power injected into the grid. The grid power flow and cumulative current controls are identical to that in any single converter system and will be not discussed here. In steady state, if the winding resistances are neglected, the voltage equations of the cumulative sub-system written in the grid voltage vector oriented d,q frame are:

$$V_{\Sigma d}\approx V_s-\omega_s L_t N I_{\Sigma q} \qquad V_{\Sigma q}\approx \omega_s L_t N I_{\Sigma d} \tag{24}$$

The cross currents can be used to trim the individual converter active power flows (balancing). The voltage and current components of the cross sub-system are linked via the leakage inductance matrix. In steady state, after neglecting the windings resistive voltage drops, the voltage equations describing the cross sub- system (in the grid voltage vector oriented d,q frame) are:

$$\left[\Delta v_d\right]\approx -\omega_s\left[L_\sigma\right]\left[\Delta i_q\right] \qquad \left[\Delta v_q\right]\approx \omega_s\left[L_\sigma\right]\left[\Delta i_d\right] \tag{25}$$

For optimal system operation, deviations of the converter dc bus voltages from the average value:

$$\Delta v_{dc\,i}=v_{dc\,i}-v_{dc\,ave} \qquad i=1:N \qquad v_{dc\,ave}=1/N\sum_{i=1}^{N} v_{dc\,i} \tag{26}$$

should be minimized. Balance of the individual converter dc bus voltages can be actively controlled by redistributing the total power flow created by the cumulative active current component. This can be accomplished by controlling the fundamental comments of the cross currents and related cross-power flows by the dc bus balancing controller shown in Fig. 3. Based on differences of the converter dc bus voltages from their average value, the balancing controller sets the cross-power flow references $\left[\Delta p\right]^{Ref}$ which are further converted into the cross current references of each converter ($\left[\Delta i_d\right]^{Ref}$ and $\left[\Delta i_q\right]^{Ref}$).

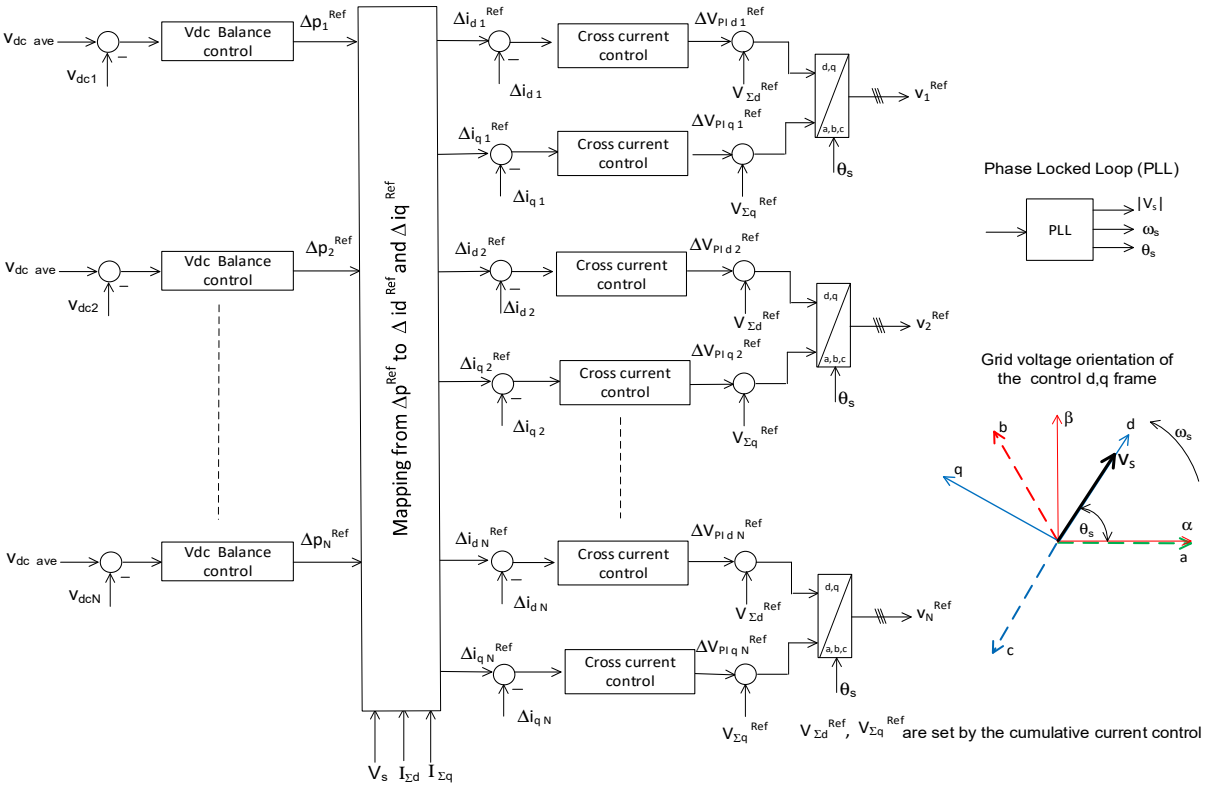

Fig. 3: The dc bus voltage balancing and cross current controls in the multi-converter system with the converters paralleled via the MWT.

Cross power flows and stability of converter dc bus voltage balance control

In this section it will be shown that differences between the effective inductances seen by the cumulative and cross currents, which is introduced by the MWT, may have a significant impact on the power flows among the converters. In general, the converter active power is defined by the scalar product of its voltage and current vectors. In the grid voltage oriented *d,q* frame (Fig. 3, $V_{\Sigma d} = V_s$, $V_{\Sigma q} = 0$), the converter active powers grouped into the power vector [p] are ($[I]$ is $N \times N$ unity matrix):

$$\begin{aligned}&[p] = -3/2[\Delta v]^T[\Delta i] = \\ &-3/2\left\{ \left(V_{\Sigma d}[I] + [\Delta v_d]^T\right)\left(I_{\Sigma d}[I] + [\Delta i_d]\right) + \left(V_{\Sigma q}[I] + [\Delta v_q]^T\right)\left(I_{\Sigma q}[I] + [\Delta i_q]\right)\right\}\end{aligned} \tag{27}$$

From (27) it is possible to separate the active power exchanges among the converters $[\Delta p]$:

$$[\Delta p] = -3/2\left\{ V_{\Sigma d}[\Delta i_d] + V_{\Sigma q}[\Delta i_q] + [\Delta v_d] I_{\Sigma d} + [\Delta v_q] I_{\Sigma q}\right\} \tag{28}$$

This equation for the active power flows produced by the cross currents (28) can be expanded by introduction of the voltage equations (25). The expanded form is ($V_{\Sigma d} = V_s$):

$$[\Delta p] = -3/2\left\{V_s[\Delta i_d] - \omega_s\left(L_t N[I] - [L_\sigma]\right)\left(I_{\Sigma q}[\Delta i_d] - I_{\Sigma d}[\Delta i_q]\right)\right\} \tag{29}$$

Conventionally the active cross current components $[\Delta i_d]$ are used to control the cross-power flows (power exchanges among converters) while the reactive components of the cross currents are kept at zero ($[\Delta i_q] = 0$). Then (29) is reduced to the following form:

$$[\Delta p] = -3/2\left\{V_s[I] - \omega_s\left(L_t N[I] - [L_\sigma]\right) I_{\Sigma q}\right\}[\Delta i_d] \tag{30}$$

In this cross-power vector equation (30) there two terms can be distinguished:

- the first or principal term, proportional the grid voltage ($V_s[I]$) and the *d* axis cross currents.
- the second or parasitic term, defined by the cumulative mode reactive current and the transformer leakage inductance matrix (cross-coupling effect).

It should be emphasised that the second term is proportional to the cumulative mode reactive current. Thus, it can change its sign when character of the reactive current injection changes from the inductive (+sign) to capacitive (-sign). As the result, when the converters perform reactivate power injection, the cross-power flow among the converters is not defined by a simple scaling of $[\Delta i_d]$ by the factor $3/2V_s$ but by a matrix. Effectively in the $[\Delta p]^{Ref}$ to $[\Delta i_d]^{Ref}$ mapping we must consider effects of the parasitic cross coupling term (proportional to $I_{\Sigma q}$):

$$3/2\{V_s[I]-\omega_s(L_t N[I]-[L_\sigma])I_{\Sigma q}\} \qquad \text{where } [I] \text{ is a } N\text{x}N \text{ identity matrix} \tag{31}$$

If effect of the second term (cross-coupling) can be neglected, the *d* axis cross current references can be derived from the cross-power references using the following simple mapping (with $[\Delta i_q]^{Ref}=0$):

$$[\Delta i_d]^{Ref} = -[\Delta p]^{Ref}/(3/2V_s) \tag{32}$$

Otherwise, as far as the diagonal term in (31) $V_s[I]$ remains dominant, the cross-coupling in (31) does not cause power flow sign inversions and hence the active control of the dc bus voltage balance remains stable. Changes of the reactive current injection $I_{\Sigma q}$ may alter the control loop gains and dynamic performances but they will not lead to the control instabilities. To guarantee stability, the matrix $V_s[I]-\omega_s(L_t N[I]-[L_\sigma])I_{q\Sigma}$ must be positive-definite or at least semi-definite. To fulfil that requirement the reactive (capacitive) cumulative current must satisfy the following criterion [9]:

$$I_{\Sigma q} \geq -V_s/(\omega_s(\lambda_{\max}-NL_t)) \quad (\lambda_{\max} \text{ is the largest eigenvalue of the cross-inductance matrix } [L_\sigma]) \tag{33}$$

If this (capacitive) current limit is violated the balancing control will become unstable due to power flow sign inversions in the eigen direction associated to $\lambda_{\max}$ [9]. By inspection of (29) it is possible to observe that the cross-coupling term in the cross-power equation is possible to eliminate when the converters are operating with nonzero power factors. For that the active and reactive components of the cross currents must be simultaneously controlled using the following map:

$$[\Delta i_q]^{Ref} = I_{\Sigma q}/I_{\Sigma d}[\Delta i_d]^{Ref}; \qquad I_{\Sigma q}[\Delta i_d]-I_{\Sigma d}[\Delta i_q]=0; \qquad [\Delta i_d]^{Ref}=-[\Delta p]^{Ref}/(3/2V_s) \tag{34}$$

This option is obviously feasible when the $I_{\Sigma q}/I_{\Sigma d}$ ratio is low (operation with high power factors).

Example case

In the example case presented in this section a multi-converter system shown in Fig. 1b is considered. It is consisted of *N*=6 converters coupled with the 33kV/50Hz power grid via a 18 MVA MWT with 33kV HV/6 × 2.25kV LV windings. The transformer short circuit voltages are given in Table 2.

Table 2: MWT relative short circuit voltages/impedances (in % of single LV winding base).

Single LV Winding Power Base		Short-circuited Winding						
		HV	LV1	LV2	LV3	LV4	LV5	LV6
Energized Widing	HV							
	LV1	51,9%						
	LV2	30,5%	30,6%					
	LV3	19,7%	64,1%	30,6%				
	LV4	19,6%	96,0%	64,1%	30,6%			
	LV5	30,4%	127,4%	96,0%	64,1%	30,6%		
	LV6	51,6%	159,8%	127,9%	96,0%	64,1%	30,6%	

The short circuit voltages are used to construct the leakage inductance matrix $[L_\sigma]$ ($L_{base}=5.37\times10^{-3}$ H):

$$[L_\sigma]=\frac{5.37\times10^{-3}}{100}\begin{bmatrix} 51.9\% & 25.9\% & 3.75\% & -12.3\% & -22.6\% & -28.9\% \\ 25.9\% & 30.5\% & 9.8\% & -6.9\% & 17.6\% & -22.9\% \\ 3.75\% & 9.8\% & 19.7\% & 4.4\% & -7.0\% & -12.4\% \\ -12.3\% & -6.9\% & 4.4\% & 19.6\% & 9.7\% & 3.5\% \\ -22.6\% & 17.6\% & -7.0\% & 9.7\% & 30.4\% & 25.7\% \\ -28.9\% & -22.9\% & -12.4\% & 3.5\% & 25.7\% & 51.6\% \end{bmatrix} \tag{35}$$

Once $[L_\sigma]$ is defined the total transformer leakage impedance for the cumulative system is found to be $NL_t \approx 18$ % (from eq. (12),(14) and (21)). Also, the eigen-values $[\lambda]$ of the matrix $[L_\sigma]$ are found:

$$[\lambda] = eig([L_\sigma]) = \frac{5.37\times10^{-3}}{100} diag([7.3\% \quad 9.6\% \quad 16.2\% \quad 18.0\% \quad 32.1\% \quad 120.6\%]) \tag{36}$$

The highest eigen-value $\lambda_{\max} = \max([\lambda])$ is approx. 120% of the single LV winding base (notice it is higher than 1 p.u.!). It defines the critical capacitive reactive current/power injection beyond which the dc bus voltage balancing instability is lost. From (33), and if the lowest value of the grid voltage of 80% of V_{sn} is assumed, it is possible to theoretically predict that the balancing control will become unstable when the capacitive reactive power/current injection exceeds the critical value of:

$$I_{\Sigma q} = -V_s / \left(\omega_s \left(\lambda_{\max} - NL_t\right)\right) = -0.8\,p.u. / \left(1.2\,p.u. - 0.18\,p.u\right) = -0.784\,p.u.\,(604\,Arms / 854\,Apeak, Q = -11.3MVAr) \tag{37}$$

This theoretical result, which predicts instability in the converter dc bus voltage balancing control when capitive current injection exceeds 11.3MVAr, has been confirmed in PLECS simulations using the MWT model created using the standard PLECS coupling inductor model which permeates are defined as explained by the matrix $[L_{MWT}]$ (17). The simulation results shown in Fig. 4 depicts evolutions of the total converter active and reactive powers, currents, and dc bus voltages when the converter total reactive (capacitive) current/power injection is increased from -5.3 MVAr to -13.3 MVAr in three steps. The active power flow has been maintained at constant, relatively low, value of 3.4 MW. It can be observed that, when the reactive power injection reaches -13.3MVAr (the theoretical limit), the converter individual dc buss voltages start diverging (while their average value remains stable), exactly as predicted by the theoretical result (37). Due to low active power transfer (low power factor), stabilization via compensation of the cross-coupling using $[\Delta i_q]$ has not been utilized ($[\Delta i_q]^{Ref}$ set to 0).

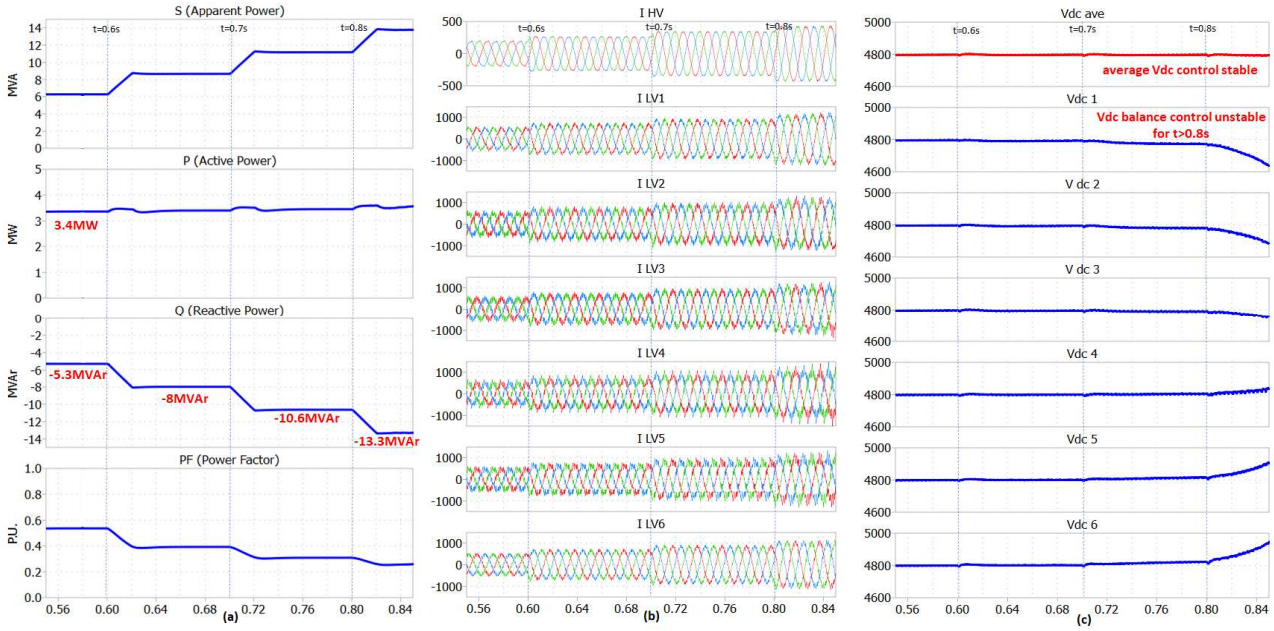

Fig. 4: Converter powers, currents and dc bus voltages. Divergence of the individual converter dc bus voltages starts when the reactive (capacitive) current injection exceeds the critical value of 0.784 p.u. (604Arms, 854Apeak).

Conclusions

High power converters can be constructed by using several VSC converters which are mutually paralleled via MWTs. If the converter dc busses are not mutually interconnected, balance of their dc bus voltages must be actively controlled. The active balancing control of the dc bus voltages is

conventionally achieved by trimming the active power flows of the converters via control of active components of the cross currents at the fundamental frequency. However unexpected stability issues with the active dc voltage balance control may been encountered in the operational points characterized by low capacitive power factors and depressed grid voltages. This is particularly the case when MWTs are designed to provide high leakage reactance between the secondary windings (often exceeding 100%) to minimize the PWM switching current ripple.

In the theoretical analysis presented the origin of potential instabilities in the active balancing control has been explained. It has been linked to large differences in the effective inductances in the cumulative and cross currents paths which may is created by magnetically coupled MWT windings. While such high inductance asymmetry is desirable for minimization of the cross current ripple caused by the PWM interleaving and voltage drops in the cumulative current path, it also creates strong cross coupling terms proportional to the cumulative reactive current injection in the mapping of the cross currents into the cross-power flows. It has been theoretically shown that, if a critical level of the capacitive reactive current injection is exceeded, these cross-coupling terms may alter signs of the cross-power flows and thus destabilise the active dc bus voltage balancing control. This type of instability of the dc bus voltage balancing control has been confirmed by the simulation result presented.

The destabilizing cross coupling can be effectively eliminated, and the dc bus voltage balancing control stabilized, in operational points characterized by higher power factors. For that, it has been proposed to simultaneously control the active and reactive components of the cross currents. Due to the paper size limitations, evaluation of the performance of this compensation method was not included in this paper.

References

[1] H. Akagi, A. Nabae, S. Atoh, 'Control Strategy of Active Power Filters Using Multiple Voltage-Source PWM Converters, IEEE Transactions on Industry Applications, May/June 1986, Vol. IA-22, Issue 3, pp. 460-465.

[2] T. Konishi; S. Hase, A. Okui, S. Kinoshita, M. Sonetaka, 'Development of PWM converter with large capacity for electric railway substation', The Fifth International Conference on Power Electronics and Drive Systems, 2003. PEDS 2003, pp. 1264-1267.

[3] J. Chivite-Zabalza, M. Á. R. Vidal, Izurza-Moreno, G. Calvo, D. Madar, "A Large-Power Voltage Source Converter for FACTS Applications Combining Three-Level Neutral-Point-Clamped Power Electronic Building Blocks", IEEE Transactions on Industrial Electronics, Vol. 60, Issue 11, Nov. 2013, pp. 4759-4771.

[4] M. Morati, D. Girod, F. Terrien, V. Peron, P. Poure, S. Saadate, "Industrial 100-MVA EAF Voltage Flicker Mitigation Using VSC-Based STATCOM With Improved Performance", IEEE Transactions on Power Delivery, Vol. 31, No. 6, Dec. 2016, pp. 2494-2501.

[5] G.R. Walker, "Digitally-Implemented Naturally Sampled PWM Suitable for Multilevel Converter Control", IEEE Transactions on Power Electronics, Vol. 18, Issue 6, Nov. 2003, 1322-1329.

[6] D. Zhang; F. Wang; R. Burgos; R. Lai; D. Boroyevich, 'Impact of Interleaving on AC Passive Components of Paralleled Three-Phase Voltage-Source Converters', IEEE Transactions on Industry Applications, Vol. 46, Issue 3,,May-June 2010, pp. 1042 – 1054.

[7] I. G. Park, S. I. Kim, "Modelling and Analysis of Multi-Interphase Transformers for Connecting Power Converters in Parallel", 28th IEEE Power Electronics Specialists Conference. PESC97, 1997, pp. 1164-1170.

[8] J. Wang; A.F. Witulski; J. L. Vollin; T.K. Phelps; G.I. Cardwell, 'Derivation, calculation and measurement of parameters for a multi winding transformer electrical model', Fourteenth IEEE Annual Applied Power Electronics Conference and Exposition, APEC '99, 1991, Vol. 1, pp. 220-226.

[9] D. Basic; H. Baërd; S. Siala, 'Instability in Active Balancing Control of DC Bus Voltages in STATCOM Converters Paralleled via Interphase Transformers', IEEE Transactions on Power Delivery, Vol. 36, Issue 4, Aug. 2021, pp. 1992 – 2000.

[10] AESO, 'Transformer Modelling Guide', Revision 2, 2014, available on-line at https://www.aeso.ca/assets/linkfiles/4040.002-Rev02-Transformer-Modelling-Guide.pdf.

[11] J. El Hayek, 'Modeling aspects for power conversion locomotive transformers', 2010 IEEE Region 8 International Conference on Computational Technologies in Electrical and Electronics Engineering (SIBIRCON), 2010, pp. 513-517.

[12] M. Dudzik, A. Kobielski; J. Prusak, S. Drapik, 'Traction transformers, selected difficulties in object identification', International Symposium on Power Electronics Power Electronics, Electrical Drives, Automation and Motion, SPEEDAM, 20-22 June 2012, pp. 802-805.